Morphology of melt-crystallized poly(vinylidene fluoride): influence of

Morphology of melt-crystallized poly(vinylidene fluoride): influence of chain structure and polydispersity

Arun K. Nandi*

Institute of Molecular Biophysics, Florida State University, Tallahassee, FL 32306, USA

(Received 11 October 1993; revised 3 March 1994)

The morphology of melt-crystallized poly(vinylidene fluoride) (PVF_2) fractions and whole polymers is presented for a wide range of crystallization temperatures (T_c). In both cases, at each isothermal T_c an increase in size of α-spherulites with increase in head-to-head (H-H) defects of the chain was observed. However, at the same T_c, for some fractions with a higher concentration of defects (>5.27% defects) the spherulitic radius decreased with increasing defect concentration, and in some cases a disordered morphology was also observed. Possible explanations are offered for these exceptions. When quenching from the melt to room temperature, a decrease in spherulitic size with increasing H-H defect content was found for both the fractions and the whole polymers. When comparing isothermally crystallized samples under the same undercooling, similar deterioration of spherulitic size and morphology with increasing defect structure in the chain was found. A general explanation involving the inclusion of H-H defects into the lamellae is suggested. The spherulites of whole polymers are larger than those of the fractions and a possible explanation for this is offered.

(Keywords: morphology; poly(vinylidene fluoride); spherulitic size)

INTRODUCTION

Both solution-grown or melt-crystallized polymer crystals have lamellar aggregates in association with the amorphous and interfacial regions[1]. The various types of morphology, e.g. spherulitic, axiatitic, dendritic, fibrillar, etc., are produced by a suitable combination of the above primary crystals[2,3]. The morphology of crystalline polymers depends on the crystallization conditions, and under similar crystallization conditions the morphology also depends on molecular weight, branch content, co-unit content and polydispersity of the polymer[4–6].

Poly(vinylidene fluoride) (PVF_2) is an important crystalline polymer from the technological point of view, particularly for its good piezoelectric and pyroelectric properties[7]. Commercial polymers contain about 3.5–6% head-to-head (H-H) defects. The influence of H-H defect on the melting point and crystallization kinetics of PVF_2 has been reported previously[8,9]. In the present paper, the morphology of both fractions and whole polymers crystallized under similar conditions, is presented.

PVF_2 crystallizes in five different polymorphs: α, β, γ, δ and ε. The crystal structures are different for different polymorphs[7–10]. Naturally, a diversity in morphology of PVF_2 crystallized under different conditions should be observed[11–19]. Gianotti *et al.*[11] first observed three different morphologies of PVF_2 crystallized under isothermal conditions. The spherulites with high birefringence were assigned to the α polymorph and the coarse spherulites with low birefringence were assigned to the γ polymorph. The other morphological variety produced from the solid-state transformation was assigned to the β polymorph. But later studies[12–17] confirmed that the polymorph produced from solid-state transformation is the higher melting γ' polymorph, having a texture similar to that of α spherulites. Marand and Stein[18] reported the morphology of PVF_2 during isothermal crystallization in the presence of an electric field, and observed that the γ phase was produced in preference to the α phase, which is preferentially produced in the absence of an electric field. Thus the three types of morphology for the three different polymorphs of PVF_2 produced under isothermal crystallization conditions from the melt are well documented. However, in some cases a difference in morphology has been noticed between Kureha and Kynar groups of PVF_2 samples crystallized in a similar way from the melt. It has also been noticed that similar morphologies occur in Kynar group samples at crystallization temperatures (T_cs) 6°C lower than those of Kureha samples[12,15]. Lovinger's argument[15] on this dissimilarity for different amounts of H-H defects in the two groups of samples may be ambiguous because morphology is dependent on polydispersity as well. To delineate this aspect in a quantitative manner, an elaborate study using sharp PVF_2 fractions was carried out by optical microscopy and by small-angle light scattering (SALS) measurements. The use of sharp fractions of PVF_2 in the morphology study eliminates the effects of structural and molecular polydispersity present in the whole polymers, and thus helps to give a clearer understanding of the dependence of morphology on the amount of H-H defect. The dependence of PVF_2 morphology on molecular weight was determined using sharp fractions of PVF_2 with the same amount of H-H defect but differing in molecular

Address for correspondence: Polymer Science Unit, Indian Association for the Cultivation of Science, Jadavpur, Calcutta 700 032, India

0032-3861/94/24/5202-08

weight. The effect of polydispersity (both structural and molecular) was also evaluated using the unfractionated commercial polymers and comparing the morphology with those of the fractions under identical conditions.

In our earlier report[8] it was pointed out that the high crystallinity and large depression of equilibrium melting point compared to Flory's exclusion model is due to inclusion of a portion of defect into the crystalline lamella. The kinetic analysis of crystallization provides corroborating evidence in favour of this fact[9]. The present study of morphology of PVF_2 crystals allows further insight into the problem. For these investigations, sharp fractions of PVF_2 with varying amounts of H-H defect and whole (unfractionated) polymers were crystallized both in quenching and in isothermal conditions. A systematic study covering all the above aspects is presented here. In particular, attention is focused on the morphology of the α-polymorph of PVF_2.

EXPERIMENTAL

Samples

Two types of samples were used in this work: commercial PVF_2 samples (unfractionated) obtained from three chemical companies (Kureha Chemical Co., Japan, Solvey Corporation, USA, and Pennwalt Corporation, USA); and very sharp fractions of these commercial polymers obtained from fractional crystallization in dilute (0.3% w/v) solution of acetophenone. The characteristics of the samples have been reported previously[8].

Crystallization

The samples (fractions and whole polymers) were crystallized by two different procedures: quenching to room temperature (25°C) and isothermal crystallization. In the first case, the polymer films (compression moulded, 50–60 μm thick) were melted at 227°C and then quenched to room temperature. In the isothermal crystallizations, small pieces of polymer film (50–60 μm thick) were taken on microscope slides (0.65 cm wide and 7.5 cm long) with a portion of microscope cover glass on the film. These microscope slides were introduced into glass tubes, evacuated to 100–150 μmHg and sealed. They were melted in a thermostatic oil bath set at 227°C for 10 min to destroy all the nuclei[19,20] and then quickly transferred to the other thermostatic oil bath set at a predetermined T_c. Sufficient time for complete crystallization was given to each sample at each T_c; the approximate times of crystallization were chosen from the upper flat portion of the crystallization isotherms of the respective or analogous samples at those T_cs[9]. After completion of the process they were cooled to room temperature and the sample slides were taken out from the tubes. Of course, it is pertinent to mention here that after cooling to room temperature from the isothermal crystallization conditions, crystallinity does not change much (it increases by $\sim$5%) and so almost all morphological properties arising from isothermal crystallization are fully retained. (The crystallinity attained for PVF_2 samples at the flat portions of crystallization isotherms is $\sim$50%. During cooling of these isothermally crystallized samples to room temperature, another 5% increase in crystallinity occurs[9]. This slight increase in crystallinity does not affect the morphology because the spherulites produced in this condition are much smaller than those of the isothermal condition.)

Microscopy

A Leitz Metallux II microscope fitted with an automatic camera system was used in this work. The sample slides were viewed under perfectly crossed polarizers with a 40 × magnification eyepiece or, in some cases, a 10 × magnification eyepiece. For measurement of the spherulitic radius the micrometre scale was photographed in the same resolution as used for the morphology study. The radii of about 10 spherulites were measured and an average was taken to obtain the average spherulitic radius.

Small angle light scattering

The H_v SALS patterns were taken from a photometer similar to that described by Stein[22]. The wavelength of light used was 632.9 nm. Polaroid 55 films were used to take instant pictures. The average spherulitic radius (R) was measured from the relation[4] $4\pi(R/\lambda)\sin(\theta/2)=4.1$, where θ, the scattering angle, was measured from the ratio of distance of maximum intensity from the centre to the distance of the photographic film from the sample.

RESULTS AND DISCUSSION

Morphology of fractions

The micrographs of PVF_2 fractions isothermally crystallized at 155°C are presented in *Figure 1*. The general features of this figure are that in each micrograph the spherulites with higher birefringence are α spherulites and the coarse spherulites with low birefringence are γ spherulites. The banded nature of α spherulites is clearly seen, and was also observed by Lovinger[15] from electron microscopic study of unfractionated PVF_2 samples.

The morphology of fractions having the same amount of defect structure but differing in molecular weight will be discussed first, and the fractions Sol-5, Sol-6 and Sol-7 were chosen for this purpose. These samples have almost the same defect concentration (4.02–4.1 mol%) but the molecular weights ($\bar{M}_v$) are 4.6×10^5, 5.9×10^5 and 7.0×10^5, respectively. From *Figure 1* it is apparent that the sizes of α spherulites are almost the same for these three fractions and this is also true for other T_cs (*Table 1*). This indicates that the molecular weight does not have much influence on the morphology of PVF_2 fractions crystallized isothermally for the molecular weight range studied here. However, the γ spherulites increased in number as the molecular weight increased at higher T_cs.

The influence of structural irregularity on the morphology of isothermally crystallized PVF_2 fractions will now be examined. For this purpose, $T_c=155$°C was chosen first because at this T_c PVF_2 fractions with a wide range of H-H defect contents crystallize isothermally. A glance at the micrographs in *Figures 1a–h* clearly reveals that with increasing H-H defect concentration of the fractions, the spherulitic size increases. Although crystallization times were different in some cases, this does not affect the final morphology, as apparent from *Figures 1b* and *c* of the KF-7 fraction. At higher T_cs, although there is time-dependent solid-state transformation from the α to the γ' phase, the identical morphology of the two phases does not affect the final morphology at all[16,17]. The α spherulites seen in

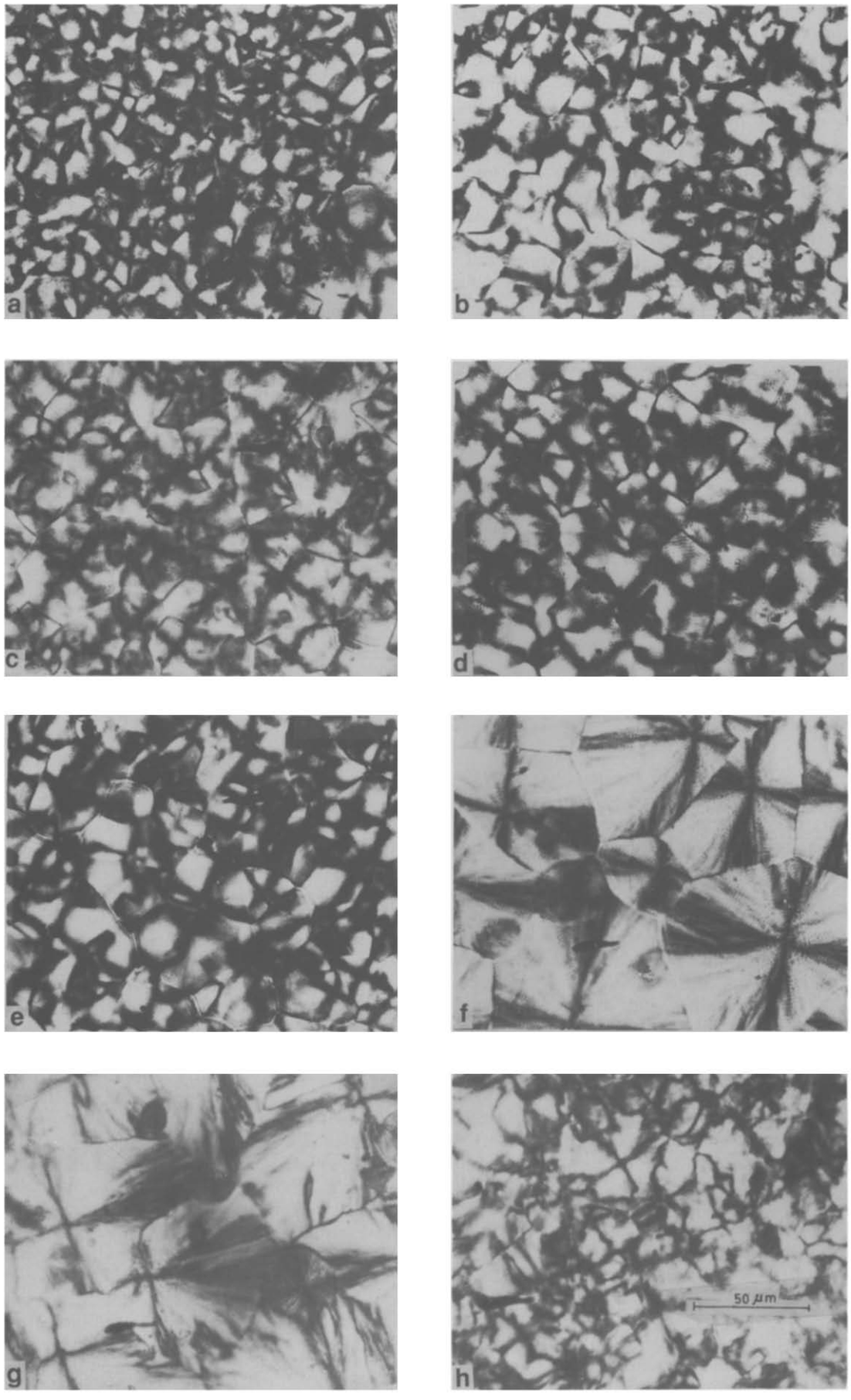

Figure 1 Photomicrographs of PVF_2 fractions isothermally crystallized at 155°C. (a) Defect = 3.36% for 1 day; (b) defect = 3.61% for 1 day; (c) defect = 3.61% for 65 h; (d) defect = 4.02% for 1 day; (e) defect = 4.1% for 1 day; (f) defect = 4.99% for 64 h; (g) defect = 5.27% for 7 days; (h) defect = 5.54% for 9 days. All micrographs are at same scale (see scale bar in (h))

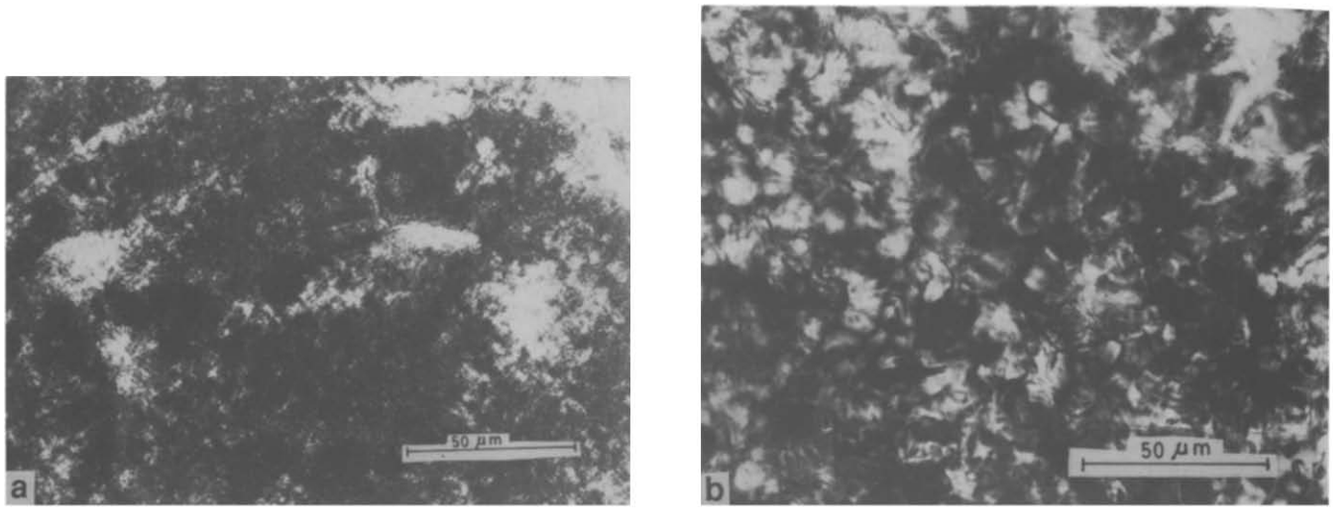

Figure 2 Typical micrographs of (a) defect = 5.48% quenched to room temperature (no well developed morphology); and (b) defect = 5.54% crystallized at 146°C for 1 day (disordered morphology)

Table 1 Spherulitic radii of PVF_2 fractions for quenching to 25°C and isothermal crystallization temperatures

Sample	H-H defect (mol%)	Spherulitic radius (μm) at							
		Quenching to 298 K[a]	413 K	419 K	425.5 K	428 K	433 K	437 K	440 K
KF-5	3.33	5.0	–	–	–	12	22	35	52
KF-6	3.36	5.0	–	–	–	11	28	42	–
KF-7	3.61	4.5	–	–	–	16	27	51	–
Sol-5	4.02	4.0	–	–	–	17	34	55	66
Sol-6	4.07	4.0	–	–	–	19	32	61	nc
Sol-7	4.10	4.0	–	–	–	18	35	53	nc
KY-3	4.91	2.7	–	–	–	18	35	53	nc
KY-4	4.99	2.7	–	10	16	39	54	nc	nc
KY-5	5.27	–	–	7	24	43	nc	nc	nc
KY-6	5.48	–	11	dm	19	25	nc	nc	nc
KY-7	5.54	–	dm	dm	15	17	nc	nc	nc

dm = Disordered morphology; nc = not crystallizable within 2 weeks
[a] From SALS data

Figures 1f and *g* are somewhat coarser than those of the predecessors, and the ring spacing appears to be larger than the other ringed spherulites. γ spherulites are also present here. The coarseness of spherulites is usually explained from the D/G parameter (δ), where D is the diffusion constant of the crystallizing unit to the crystal surface and G is the growth rate. The coarseness increases if the ratio δ increases [2,3]. For samples with higher H-H defect content, at any T_c the growth rate is lower than for samples with lower H-H defect content[9]. Assuming that D is the same for fractions with the same defect content, the lower G values for samples with higher defect content increases the ratio D/G, disfavouring the small-angle dendritic branching required for the formation of good spherulites. Again, in *Figure 1h* the α spherulites are small and some disordered morphology is also observed.

The results of morphological study are summarized in *Table 1*. At the quenching condition the spherulitic radii were determined from SALS experiments. However, for defect concentrations >5.27%, no characteristic scattering was observed in SALS experiments. The corresponding micrographs showed no well-developed spherulites. Disordered morphology was also noted at some isothermal T_cs. Representative micrographs of these two categories are presented in *Figure 2*.

In *Figure 3* the spherulitic radius of the α phase of PVF_2 fractions is plotted against H-H defect content for different T_cs. In general, at each T_c the spherulitic radius increases with increase in defect concentration except at $T_c = 155$ and 152.5°C, where maxima in the plots at a defect concentration of ~5.3% are observed. The increase in spherulitic size with increase in H-H defect concentration at a given T_c can be explained on the basis of undercooling. It was established previously that the equilibrium melting temperature (T_m) decreases with increase in H-H defect content[8]. So in spite of the fractions remaining at the same T_c, the fractions with higher H-H defect content experience lower undercooling compared to the samples with lower defect content. The nucleation density, therefore, is low for samples with higher defect content, and this causes larger spherulites for samples with higher H-H defect content at a given T_c.

An exception to the above assertion is for defect concentration >5.27%, for which a decrease in spherulitic radii with increase in H-H defect content was observed.

According to Keith and Padden[22], proliferation of fibrils occurs due to non-crystalline (or less easily crystallizable) impurities at the liquid–solid interface of growing fibrils. The thickness of the impurities, δ, governs the texture of the spherulites, as discussed earlier, and increasing H-H defects in the chain yields coarser spherulites. But if some impurities enter into the lamella, further growth of the lamella is prevented due to lack of adequate symmetry and cohesive forces needed for crystallization. Thus spherulites stop growing before impingement with other spherulites. In the empty space of the melt, therefore, further nucleation produces smaller spherulites. There is strong evidence[8,9,23,24] that H-H defects enter into the crystalline lattice of PVF_2. So with more H-H defects in the chain, some defects will enter into the lamella; the gradual increase of defect concentration in the lamella prevents its further growth resulting in smaller spherulites. The distribution of spherulitic size observed in *Figure 1h* is also larger than its predecessors, for the reason mentioned above. However, PVF_2 with a higher H-H defect content may also produce a completely disordered morphology because of such inclusions. Under quenching conditions, the decrease of spherulitic radii with increase in H-H defect concentration may also be due to the reason stated above.

The morphology of PVF_2 fractions with the same undercooling will be discussed now. One would expect the same average spherulitic radii under the same undercooling for all fractions, whatever the H-H defect content, because the nucleation density is the same at that condition for all the fractions[25,26]. The results are presented in *Table 2*, where the undercooling was calculated taking T_m° values of the α phase of fractions reported in ref. 8. The results are quite different from those expected, and it is clear that under the same undercooling the spherulitic radius decreases with increase in defect concentration in all cases.

Figure 4 shows plots of the undercooling required to obtain the same size spherulites, *versus* H-H defect content of PVF_2 fractions. It is clear that the plots are parallel and this indicates that there is some common cause that hinders the formation of the same size spherulites under the same undercooling. It is also clear that to obtain the same size spherulites, samples with higher defect content required lower undercooling than samples with lower defect content. It is noteworthy that the slopes of these lines are 0.54 while the slope of the line of T_m° *versus* H-H defect concentration of fractionated

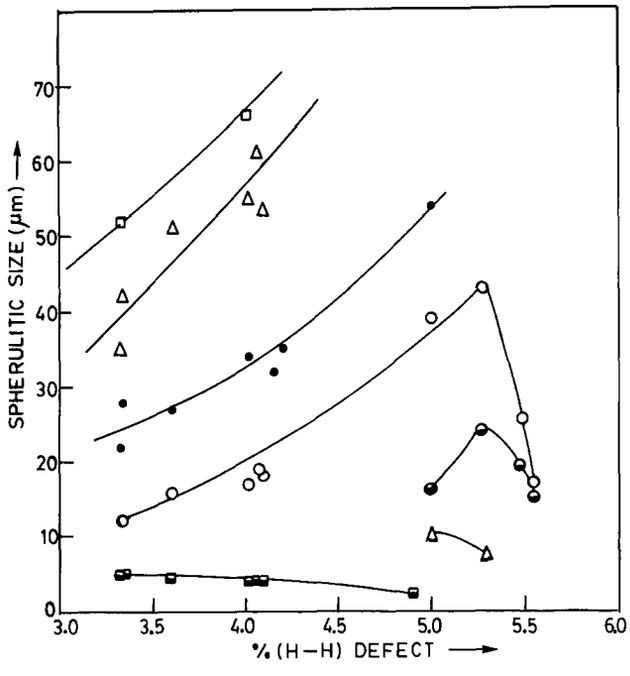

Figure 3 Plot of spherulitic size of α phase of PVF_2 fractions *versus* H-H defect concentration. For isothermally crystallized temperatures: □, 167°C; △, 164°C; ●, 160°C; ○, 155°C; ○, 152.5°C; ▲, 146°C; ■, quenching at 25°C

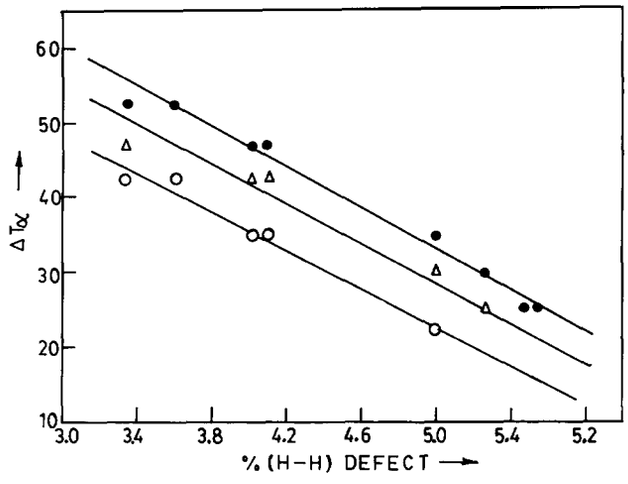

Figure 4 Plot of undercooling from α phase versus H-H defect concentration of PVF_2 fractions for the same size of α spherulites: ●, 15 ± 3 μm; △, 38 ± 3 μm; ○, 52 ± 2 μm

Table 2 Average spherulitic radii of α phase of PVF_2 fractions under same undercooling

Undercooling $[\Delta T=(T_m^0-T_c)]$ $\Delta T \pm 2$	Average spherulitic radius (μm) (H-H defect (mol%))							
	KF-6 (3.36)	KF-7 (3.61)	S-5 (4.02)	S-7 (4.1)	KY-4 (4.99)	KY-5 (5.27)	KY-6 (5.48)	KY-7 (5.54)
53.0	11	16	–	–	–	–	–	–
47.0	42	27	17	18	–	–	–	–
42.5	52	51	34	35	10	–	–	–
35.0	nc	nc	55	53	16	7	11	dm
30.0	nc	nc	nc	nc	39	24	dm	dm
25.0	nc	nc	nc	nc	54	43	19	15(dm)
21.0	nc	nc	nc	nc	nc	nc	25	17(cs)

cs = Coarse spherulite; dm = disordered morphology; nc = not crystallizable within 2 weeks

samples of the α-phase[8] is 0.58. From this similarity it can be argued that the factors which decrease the equilibrium melting temperature, by a greater amount than predicted from Flory's equilibrium theory of copolymer crystallization[27,28], also decrease the spherulitic size with increase in H-H defect content under the same undercooling. It has been proposed previously that the relative proportion of H-H defects in the crystalline and amorphous zones causes the large anomalous depression in the equilibrium melting point for samples with different H-H defect content[8]. Here, also, the relative proportion of H-H defects in the crystalline and amorphous zones causes the decrease in spherulitic size with increase in H-H defect concentration by the mechanism proposed earlier.

Whole (unfractionated) polymers

The morphology of whole PVF_2 samples is especially important to consider in order to observe the influence of structural polydispersity (i.e. wide range of H-H defect concentration) on the morphology of the above polymers. In *Figure 5*, micrographs of PVF_2 whole polymers isothermally crystallized at 145°C are presented. From the micrographs it is clear that the spherulitic size increases with increase in H-H defect content, as observed in the PVF_2 fractions. In *Table 3* the spherulitic radii of the whole polymers crystallized at different temperatures are shown. From a comparison of *Tables 1* and *3* it is clear that the spherulitic radii of whole polymers are larger than those of the fractions. Like the fractions, the whole polymers exhibit ringed spherulites except in a few cases, e.g. for KY-201 at $T_c = 159$°C and for Sol-1012 at $T_c = 164$ and 167°C. The γ spherulites were more abundant for samples with higher defect content at a given T_c, as in fractionated samples. Also, the α spherulites of samples with higher H-H defect content are coarser than those of samples with lower defect content, for the same reason as for the fractions. However, no disordered morphology was observed for the whole polymers. The better morphologies of unfractionated polymers compared to fractions with the same irregularity is common to most polymers[5,6]. In *Figure 6* the spherulitic sizes of whole polymers are plotted against defect concentration, and at each T_c there is a rise in spherulitic size with increase in H-H defect content. However, no maxima were observed in these samples. The increase in spherulitic size can be explained as discussed earlier.

In *Table 4* the spherulitic radii of whole polymers at the same undercooling are presented; the undercoolings were calculated from the T_m° values of the α phase of whole PVF_2 samples[8]. Here, as for the fractions, spherulitic size decreases with increase in H-H defect of

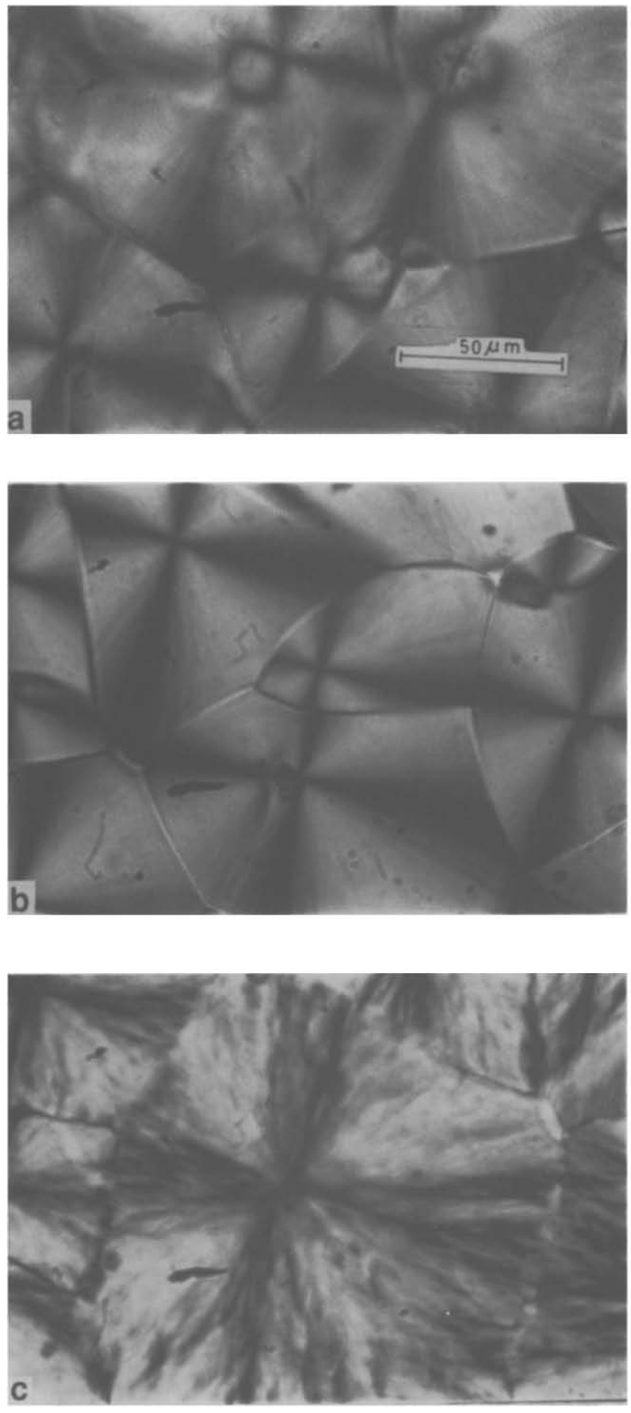

Figure 5 Photomicrographs of unfractionated PVF_2 samples crystallized at 155°C for 6 days. H-H defect concentration: (a) 3.5%; (b) 4.06%; (c) 5.31%. All micrographs are at same scale (see scale bar in (a))

Table 3 Average spherulitic radii of commercial PVF_2 samples (unfractionated) crystallized at quenching and isothermal conditions

Sample	H-H defect (mol%)	Sperulitic radius of α phase of PVF_2 (μm)							
		Quenching to 298 K[a]	413 K	419 K	425.5 K	428 K	432 K	437 K	440 K
KF-1000	3.5	5.4	–	–	–	43	54	61	120
Sol-1012	4.06	4.1	–	–	–	49	96	118	145
KY-201	5.31	2.9	9	13	30	61	110	nc	nc

nc = Not crystallizable within 2 weeks
[a] From SALS experiments

the samples. The reason is the same as that described for the fractions. It is noteworthy that, if one compares the spherulitic radius of the α phase of fractions and whole polymers with the same defect concentration under approximately the same undercooling (*Tables 2* and *4*), the spherulitic sizes of whole polymers are approximately double those of the respective fractions. A probable explanation may lie in the nucleation density of the fractions and of the whole polymers. Although both are in the same undercooling state, the structurally polydisperse chains hinder each other from nucleus formation compared to the sharp fractions, where nucleation takes place easily because the chains have the same structure. This causes the nucleation density to be higher for fractions than for whole polymers. The growth is a secondary nucleation process and has a lower activation energy than the nucleation process[26]. So in this case the effect of structural heterogeneity will be less, but the growth rate of whole polymers will be slower than that of the respective fraction.

It has been observed from the study of crystallization kinetics[9] that the overall crystallization rates of whole polymers are faster than those of analogous fractions at a given T_c, but under the same undercooling the situation becomes reversed. This is because the T_m°s of whole polymers are ~5°C higher than those of fractions having the same defect concentration[8]. So at a given T_c the whole polymers are in a greater undercooling state compared to the fractions. A comparison of crystallization isotherms, at the same undercooling, of fractions and whole polymers is presented in *Figure 7*, which is compiled from the data of ref. 9. The crystallization kinetics of Sol-1012 and its fraction Sol-7 (they have almost the same H-H defect concentration and molecular weight) have been compared at the same T_c and the same undercooling. Although at the same T_c (159°C) the whole polymer has a faster rate of crystallization, at the same undercooling (comparing the two sets of isotherms at $T_c = 155$°C for the fraction and 159°C for the whole polymer, and at $T_c = 159$°C for the fraction and 163°C for the whole polymer) the crystallization rate of the whole polymer is slower than that of the fraction. Thus the nucleation density of whole polymers is lower compared to fractions and the nuclei have more space to grow before impingement. This yields larger spherulites in the whole polymers than in the fractions.

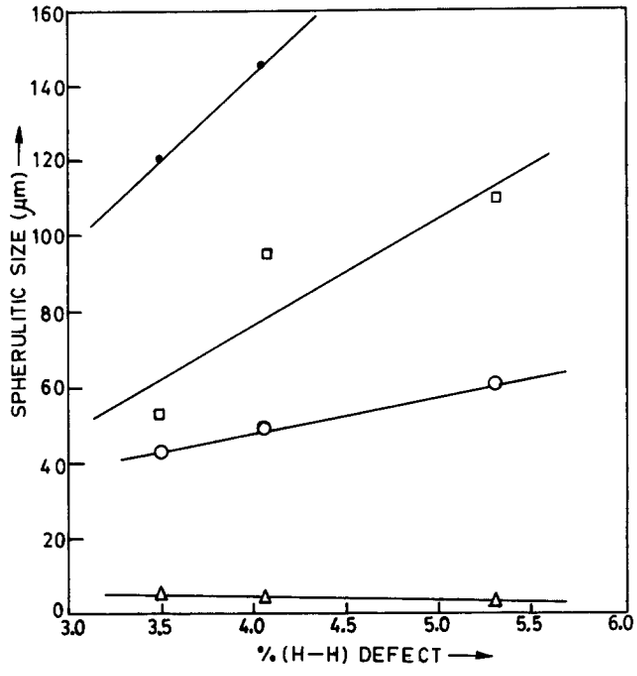

Figure 6 Plot of spherulitic sizes with H-H defect content for unfractionated PVF_2 samples at isothermal crystallization temperatures: ●, 167°C; □, 159°C; ○, 155°C; △, quenching to 25°C

Table 4 Average spherulitic radii of commercial PVF_2 samples (unfractionated) at the same undercooling

Undercooling from T_m° of α phase ($\Delta T \pm 2$)	Spherulitic radius (μm) of α phase (H-H defect (mol%))		
	KF-1000 (3.5)	Sol-1012 (4.06)	KY-201 (5.31)
58	43	–	–
54	54	–	–
50	61	49	9
45	120	96	13
38	nc	145	30
34	nc	nc	61
30	nc	nc	110

nc = Not crystallizable within 2 weeks

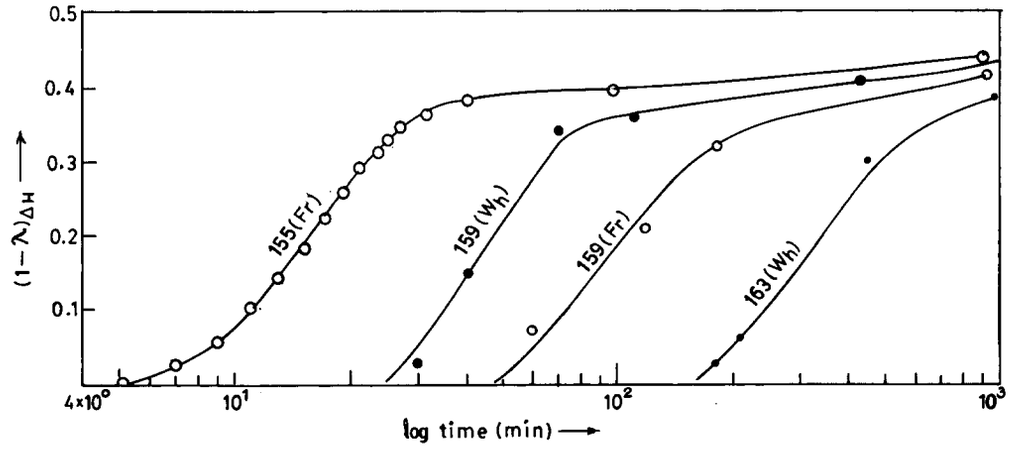

Figure 7 Crystallinity $(1-\lambda_{\Delta H})$ *versus* log(time) plots at indicated temperatures of Sol-7 fraction (Fr) (open symbols) and of Sol-1012 whole (w_h) samples (closed symbols). Data from ref. 9

In conclusion, the morphology study of PVF_2 fractions and whole polymers provides further evidence regarding the inclusion of H-H defects into the crystalline lamellae of PVF_2. Of course, the amount of H-H defect entering into the crystalline lamellae depends on the amount of H-H defect present in the chain and also on the crystallization condition. The inclusion of the defects in the lamellae causes a decrease in spherulitic size under the same thermodynamic condition of crystallization. The larger spherulitic sizes of unfractionated (structurally polydisperse) PVF_2 samples compared to those of the fractions are due to retardation of the nucleation process of whole polymers under the same thermodynamic condition of crystallization as the fractions.

ACKNOWLEDGEMENTS

The author is grateful to Professor L. Mandelkern, of Florida State University, for valuable discussion and encouragement, to Dr R. Alamo for helpful suggestions, and to the Office of Naval Research, USA, for financial assistance.

REFERENCES

1 Mandelkern, L. *Acc. Chem. Res.* 1990, **23**, 380
2 Wunderlich, B. 'Macromolecular Physics', Vol. 1, Academic Press, New York, 1973
3 Khoury, F. and Passaglia, E. in 'Treatise on Solid State Chemistry' Vol. 3 (Ed. N. B. Hannay), Plenum Press, New York, 1976, p. 335
4 Maxfield, J. and Mandelkern, L. *Macromolecules* 1977, **10**, 1141
5 Glotin, M. and Mandelkern, L. *Macromolecules* 1981, **14**, 1394
6 Mandelkern, L., Mclaughlin, K. W. and Alamo, R. G. *Macromolecules* 1992, **25**, 1440
7 Lovinger, A. J. in 'Development of Crystalline Polymers' (Ed. D. C. Bassett), Applied Science, London, 1981, p. 195
8 Nandi, A. K. and Mandelkern, L. *J. Polym. Sci., Polym. Phys. Edn* 1991, **29**, 1287
9 Nandi, A. K. and Mandelkern, L. in preparation
10 Lovinger, A. J. *Macromolecules* 1982, **15**, 40
11 Gianotti, G., Cappizzi, A. and Zamboni, V. *Chim. Industr.* 1973, **55**, 501
12 Prest, W. M. Jr and Luca, D. J. *J. Appl. Phys.* 1975, **46**, 4136
13 Prest, W. M. Jr and Luca, D. J. *J. Appl. Phys.* 1978, **49**, 5042
14 Lovinger, A. J. and Keith, H. D. *Macromolecules* 1979, **12**, 919
15 Lovinger, A. J. *J. Polym. Sci., Polym. Phys. Edn* 1980, **18**, 793
16 Lovinger, A. J. *Polymer* 1980, **21**, 1317
17 Morra, B. S. and Stein, R. S. *J. Polym. Sci., Polym. Phys. Edn* 1982, **20**, 2261
18 Marand, H. and Stein, R. S. *J. Polym. Sci., Polym. Phys. Edn* 1989, **27**, 1089
19 Weinhold, S., Litt, M. H. and Lando, J. B. *J. Appl. Phys.* 1980, **51**, 5145
20 Marand, H. L., Stein, R. S. and Stack, G. M. *J. Polym. Sci., Polym. Phys. Edn* 1988, **26**, 1361
21 Stein, R. S. 'New Methods of Polymer Characterization' (Ed. B. Ke), Wiley Interscience, New York, 1964
22 Keith, H. D. and Padden, F. J. *J. Appl. Phys.* 1963, **34**, 2409
23 Farmer, B. L., Hopfinger, A. J. and Lando, J. B. *J. Appl. Phys.* 1972, **43**, 4293
24 Lovinger, A. J., Davis, D. D., Cais, R. E. and Kometani, J. M. *Polymer* 1987, **28**, 617
25 Hoffman, J. D., Davis, T. G. and Lauritzen, J. I. Jr in 'Treatise on Solid State Chemistry', Vol. 3 (Ed. N. B. Hannay), Plenum Press, New York, 1976, p. 497
26 Mandelkern, L. 'Crystallization of Polymers', McGraw Hill, New York, 1964, p. 215
27 Flory, P. J. *J. Chem. Phys.* 1949, **17**, 223
28 Flory, P. J. *Trans. Faraday Soc.* 1955, **51**, 848